DNA Self-Assembly

Deutsche Ausgabe: DOI: 10.1002/ange.201501457
Internationale Ausgabe: DOI: 10.1002/anie.201501457

Hyperbranched Hybridization Chain Reaction for Triggered Signal Amplification and Concatenated Logic Circuits**

Sai Bi, Min Chen, Xiaoqiang Jia, Ying Dong, and Zonghua Wang*

Abstract: *A hyper-branched hybridization chain reaction (HB-HCR) is presented herein, which consists of only six species that can metastably coexist until the introduction of an initiator DNA to trigger a cascade of hybridization events, leading to the self-sustained assembly of hyper-branched and nicked double-stranded DNA structures. The system can readily achieve ultrasensitive detection of target DNA. Moreover, the HB-HCR principle is successfully applied to construct three-input concatenated logic circuits with excellent specificity and extended to design a security-mimicking keypad lock system. Significantly, the HB-HCR-based keypad lock can alarm immediately if the "password" is incorrect. Overall, the proposed HB-HCR with high amplification efficiency is simple, homogeneous, fast, robust, and low-cost, and holds great promise in the development of biosensing, in the programmable assembly of DNA architectures, and in molecular logic operations.*

In the last few decades, DNA has been employed as a powerful and fascinating material in the field of nanotechnology that enables programming of the kinetically controlled assembly of DNA nanostructures according to the Watson–Crick base-pairing principle.[1] In particular, since the advent of the hybridization chain reaction (HCR) by Dirks and Pierce in 2004, it has become a general principle to initiate successive hybridization events between two DNA hairpins to assemble nicked polymeric double helices upon the introduction of a triggering strand.[2] To date, HCR has been widely applied in the amplified detection of various bioanalytes[3] and cancer cells,[4] for the in situ mapping of mRNAs,[5] in targeted anticancer drug delivery,[6] and in the building of DNA nanostructures.[7] Moreover, diverse programming biomolecular self-assembly pathways have been proposed on the basis of HCR to form branched and dendritic DNA nanostructures.[8] However, in these systems new hairpin species were required to support the formation of corresponding nanostructures in each step, thus, the processes were not self-sustainable. Recently, LaBean et al. reported a triggered self-assembly of dendritic DNA nanostructures based on HCR for target DNA detection.[9] However, the temperature of this system had to be changed (from 25 °C to 30 °C) to facilitate the formation of dendrimers. Additionally, oligomeric structures inevitably formed while annealing the hairpin precursors, leading to the leakage of the system. More importantly, the growth process involves the spontaneous opening of a metastable stem–loop structure that has a relatively long stem (15 base pairs) at a finite rate, which may give rise to a linear growth process instead of dendritic growth. Alternatively, Xuan and Hsing developed a target triggered nonlinear HCR for the self-assembly of dendritic DNA nanostructures, which exhibited exponential growth kinetics and well-controlled system leakage.[10] However, double-stranded substrates were introduced to the system instead of hairpins, which had to be purified by forming byproducts to remove the unreacted single-stranded DNAs. Therefore, the construction of a feasible nonlinear HCR system is still a challenging task.

In biomolecular programming, the unique biological and physical properties of DNA molecules are harnessed for performing a variety of logic-gate operations as active and basic building blocks.[11] These building blocks are capable of solving computational problems by exploiting the massive parallelism in biological systems and further in bioengineering and nanomedicine. In particular, with respect to device construction, the molecular logic gates can be integrated using DNA interactions as the recognition system, which could achieve higher security for biomolecular logic circuits.[12] As a smart and interesting logic device, a keypad lock based on chemical and biomolecular systems has been developed which has attracted wide interest since it opens new opportunities to protect information against illegal invasion at the molecular level.[13] An output signal for the keypad lock is only produced when the correct inputs are introduced in the right order. That is, the "lock" is opened only when the exact "password" is known. To further boost the security systems in practical applications, such as mimicking biological systems in in vivo applications and in biomedicine to release drugs or regulate gene expression, it is highly desirable to develop more complicated keypad locks using three or more inputs at the unimolecular platform.

[*] Dr. S. Bi, Prof. Dr. Z. Wang
College of Chemical Science and Engineering
Laboratory of Fiber Materials and Modern Textiles, the Growing Base for State Key Laboratory, Shandong Sino-Japanese Center for Collaborative Research of Carbon Nanomaterials, Collaborative Innovation Center for Marine Biomass Fiber Materials and Textiles
Qingdao University, Qingdao 266071 (P.R. China)
E-mail: bisai11@126.com

M. Chen, X. Jia, Y. Dong
Key Laboratory of Sensor Analysis of Tumor Marker
Ministry of Education, College of Chemistry and Molecular Engineering, Qingdao University of Science and Technology
Qingdao 266042 (P.R. China)

[**] This work was supported by the National Science Foundation of China (21375056) and the Program for New Century Excellent Talents in University of the Ministry of Education of China (NCET-12-1024).

Supporting information for this article is available on the WWW under http://dx.doi.org/10.1002/anie.201501457.

Herein, we introduce a hyper-branched hybridization chain reaction (HB-HCR) that consists of two super-hairpin species (SH1 and SH2), two hairpins (H1 and H2), and two single-stranded assistant species (AS1 and AS2). The components could metastably coexist until exposure to a DNA initiator, triggering a cascade of hybridization events that yields hyper-branched and nicked double helices. The proposed chain-branching DNA structure growth can be used to achieve ultrasensitive detection of target DNA, and is successfully applied in the construction of concatenated logic circuits operating as a keypad lock for a biocomputing security system. The principle of our HB-HCR system is illustrated in Scheme 1. Unlike traditional hairpins with a stem-loop structure such as H1 and H2, the super-hairpin motifs with a single-stranded overhang (6 nucleotide (nt); a for SH1, e* for SH2) and a short loop (6nt; e for SH1, a* for SH2) are designed to have two bulged loops protruding in the middle of the double-stranded stem domains (c and f for SH1, g and h for SH2). It should be noted that the thermal stability of the super-hairpins is crucial to avoid spontaneous and false opening in the absence of initiator. That is, if no base pair is contained within the bulged loops, the middle loop with 16nt is long enough to allow the other strands to bind in the loop through a strand displacement reaction and further open the beacon, resulting in a false positive. Accordingly, two base pairs (bp) are designed manually in the bulged loop of the super-hairpin structure, which separate the stem into two regions, each with 16 bp. The secondary structures of the super-hairpins and hairpins are predicted and specified in Figure S1 in the Supporting Information. As a result, the super-hairpins (SH1 and SH2) and hairpins (H1 and H2) are metastable and can coexist with AS1 and AS2 until triggered by initiator (I).

Upon the introduction of the initiator (I), in the first step of the hybridization cascade the segment a* of I hybridizes and docks to the toehold a of SH1, leading to a branch migration reaction (toehold-mediated strand displacement)[14] that displaces the b part from the duplex of b/b* in SH1 with the formation of an intermediate I·SH1 (Scheme 1, reaction 1). The opened loops f and c then act as new toeholds to initiate strand displacement reactions with H1 and AS1, respectively. Briefly, the newly exposed sticky end of SH1 nucleates at the region f* of H1 and opens H1 to expose a sticky end on H1 that is identical in sequence to I. Hence, each copy of I can propagate a chain reaction of hybridization events between alternating SH1 and H1, accomplishing the traditional HCR to form a linearly growing structure. Meanwhile, the exposed loop c of the I·SH1 hybrid is available for hybridization to AS1 by binding the sticky end c*, further opening the SH1 via strand displacement (as mentioned above) and forming an $I\cdot(SH1\cdot AS1\cdot H1)_n$ complex with a single-stranded domain e–d* that is essential to the formation of the branched structure (Scheme 1, reaction 2). Analogously, domain e* of SH2 can then bind to the newly accessible toehold e, thus again initiating a branch migration to open the duplex d/d* of SH2 to yield the complex $I\cdot(SH1\cdot AS1\cdot H1\cdot SH2)_n$ (Scheme 1, reaction 3) that further hybridizes AS2 and H2 to form the first layer of the branched product (Scheme 1, reaction 4). The exposed sequence of a*–b* on SH2 is identical to I and thus it reacts with SH1 to generate the second layer of the growing branched structure with repeated units of both (SH1·AS1·H1·SH2) and (SH2·AS2·H2·SH1) (Scheme 1, reaction 5). Theoretically, this chain-branching growth would continue to form an *n*-layer branched DNA structure (Scheme 1, reaction 6). We designate this process as a hyper-branched hybridization chain reaction (HB-HCR).

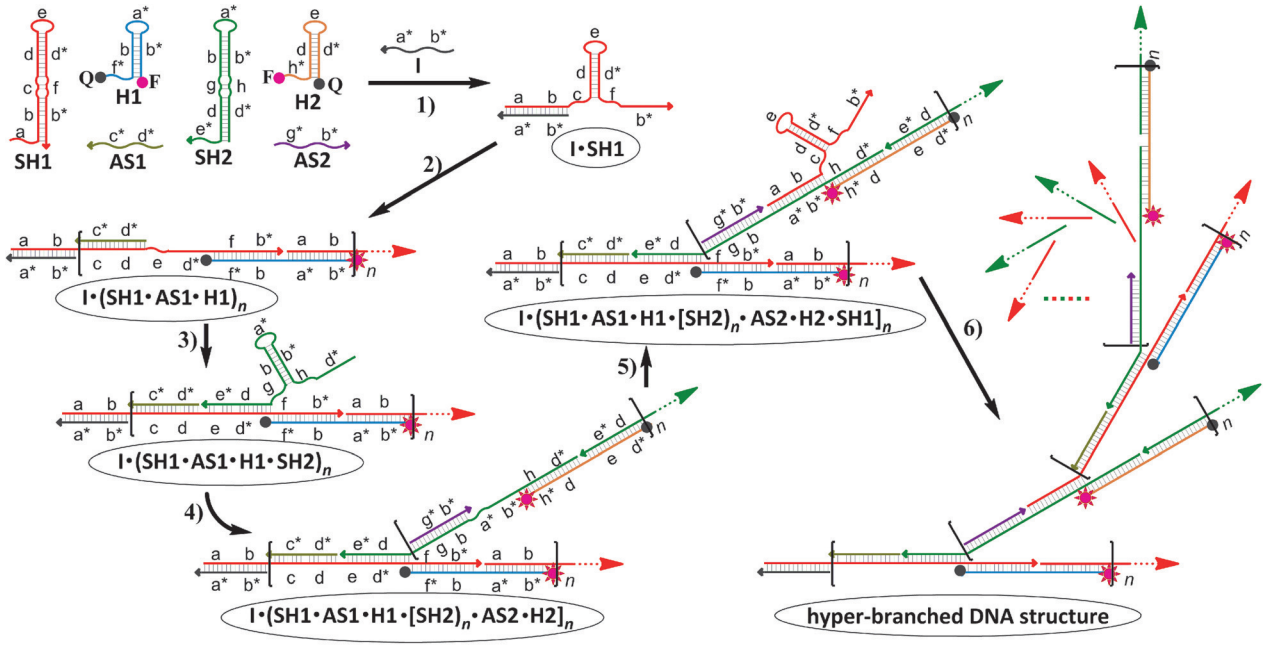

Scheme 1. Schematic representation of the components and reaction pathways for the triggered HB-HCR. Letters marked with * denote strand segments which are complementary to the corresponding unmarked domain.

Atomic force microscopy (AFM) is used to confirm the envisaged morphology of the hyper-branched DNA structure triggered by the I strand. From Figure 1 A, in the absence of I, only some tiny spots with a thickness of approximately 2 nm

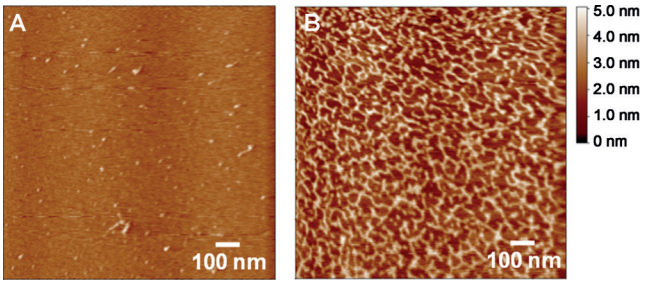

Figure 1. AFM images of the assembled products A) in the absence and B) in the presence of I (0.1 equiv). The concentration of each component is 10 μM.

are detected without seeing any assembled product. In contrast, a large amount of two-dimensional dendritic structures appear upon the addition of initiator DNA into the system (Figure 1 B). Therefore, the AFM images confirm that the proposed HB-HCR took place as anticipated, which agree with the results obtained by non-denaturing polyacrylamide gel electrophoresis (PAGE; Figure S2). Actually, it is difficult to detect the change within the solution after introduction of I (0.1 equiv) into the HB-HCR system. However, after centrifugation of the products at 10000 r min^{-1} for 1 minute, a white precipitate is evident at the bottom of the centrifuge tube, indicating the formation of large DNA structures (Figures S3 and S4).

To evaluate the growth kinetics of the HB-HCR, first additional AFM experiments of linear HCR (L-HCR) and branched HCR (B-HCR) are carried out to be able to compare the resultant products to those obtained by HB-HCR. For the L-HCR system consisting of 1 equivalent of {SH1 + H1}, linear nanowires without a branching structure are detected (Figure S5 A), corresponding to the linear polymerization between alternating SH1 and H1 in response to the addition of I (0.1 equiv). For the B-HCR system consisting of {SH1 + H1 + AS1 + SH2 + H2} (1 equiv) that is treated with I (0.1 equiv), branched DNA assemblies are formed (Figure S5 B). As anticipated, the degree of branching of the B-HCR products is significantly lower than that obtained by HB-HCR (Figure 1 B). Therefore, the AFM results of these three versions support the mechanism of the proposed HB-HCR system. Moreover, to investigate the growth kinetics of the proposed HB-HCR system quantitatively, H1 and H2 are modified with a quencher (BHQ-2) at the 3′ terminus and a fluorophore (ROX) at the 5′ terminus, respectively. Different quantities of I are introduced into the system at $t \approx 0$ and the time-dependent fluorescence intensity of ROX ($\lambda_{ex} = 576$ nm, $\lambda_{em} = 601$ nm) is measured every 2 min for 30 min at room temperature. As shown in Figure 2 A, at the beginning of the reaction, the fluorescence intensities of all cases are low because the annealed H1 and H2 in the detector remain a closed structure that brings the fluorophore

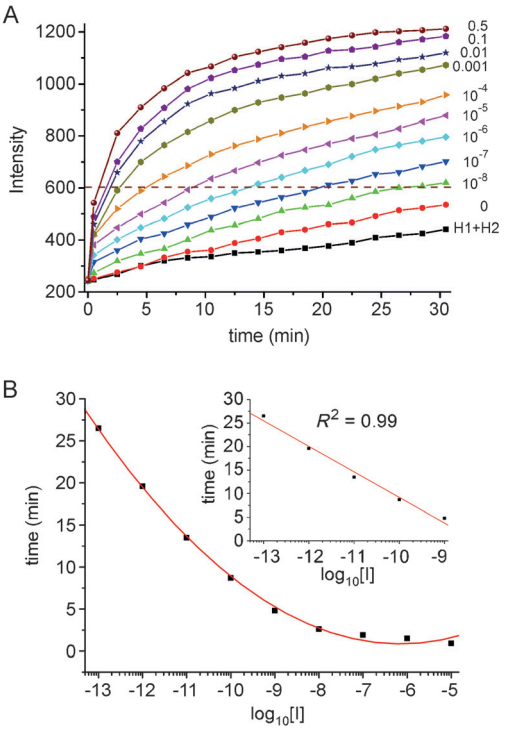

Figure 2. A) Fluorescence kinetic characterization of the HB-HCR by treating the reaction system with different amounts of the initiator I. The concentration of the species initially added is 10 μM (1 equiv). {H1 + H2} denotes the system consisting of only H1 and H2, while the plot denoted 0 is the HB-HCR system consisting of {SH1 + H1 + AS1 + SH2 + H2 + AS2} in the absence of I. The plot labels on the right-hand side denote the number of equivalents of initiator added to the reaction system. Note: 10^{-8} equiv corresponds to a concentration of 10^{-13} M. B) The time needed to reach a relative fluorescence intensity of 600 plotted against the logarithm of the initial concentration of I. Inset: linear fit of the plot when the initial concentration of I is from 10^{-13} to 10^{-9} M.

and the quencher into close proximity, resulting in an "off" fluorescence signal. This is confirmed by the control sample that consists of only H1 and H2. For the initial state, namely in the absence of I (0 equiv), since no hyper-branched DNA structure is produced as the reaction proceeds, the fluorophore never separates from the quencher. As a result, the fluorescence intensities remain at a low level throughout the experiments, indicating the species in the present HB-HCR system can metastably coexist without initiator I. The negligible fluorescence gain we attribute to system leakage caused by a few imperfectly annealed super-hairpins and hairpins.

Measurements of the kinetics of the HB-HCR over a 5×10^7-fold range of concentrations of I are further studied. Upon addition of initiator I to the system, the HB-HCR is initiated, resulting in an increase in the fluorescence intensity. We plotted the time needed to reach a relative fluorescence intensity of 600 against the logarithm of the initial concentration of I to investigate whether the HB-HCR is an exponential growth process.[8,10] From Figure 2 B, instead of a linear fit, the plot of the time needed to reach a fluorescence intensity of 600 against the logarithm of the concentration of I

shows a quadratic fit, which thus is inconsistent with exponential kinetics. However, when the initiator is at low concentration ($[I] = 10^{-8}$–10^{-4} equiv; or in terms of molarity, $[I] = 10^{-13}$–10^{-9} M), a log-linear trend in a plot of the initial concentration of I against time is obtained with a determination coefficient of $R^2 = 0.99$ (Figure 2B inset), indicating the exponential growth kinetics of the HB-HCR at low concentrations. The results imply that the growth of the hyper-branched DNA structures is affected by product inhibition, such as steric hindrance.

Importantly, the HB-HCR exhibits ultrahigh amplification efficiency for detection of initiator DNA. To make this case, error bars for three repeated experiments are added as shown in Figure S6, which verifies that the HB-HCR system can distinguish reliably between 10^{-8} equivalents of I (corresponding to a concentration of 10^{-13} M) and 0 equivalents of I within 30 min. The sensitivity is comparable to that of recently reported amplification strategies without requiring the use of any enzymes or elevated temperatures.[15] Moreover, control experiments of L-HCR and B-HCR in response to varied concentrations of initiator are carried out to confirm the growth kinetics of the HB-HCR and its ultrahigh amplification efficiency (Figures S7 and S8).

Given the cascade formation pathway for the branched DNA structure, the HB-HCR can be regarded as a network composed of concatenated YES-AND-AND logic gates as presented in Figure S9A, in which the output of one gate serves as an input for a downstream gate. In the logic circuits, three single-stranded DNA strands (as in Scheme 1), an initiator strand, and two assistant strands (AS1 and AS2) serve as inputs (inputs A, B, and C), while only SH2 is labeled with fluorophore–quencher pairs in the bulged loops as the output strand. The inputs are defined as 1 when they are present and 0 if they are absent, while the output is considered as 1 when the fluorescence signal is detected and 0 if it does not exceed a threshold value. As a result, the high fluorescence signal ("true" or "1" output) is generated after 30 min of reaction only if all of the three inputs A, B, and C are present that activate all three cascaded gates (Figure S9B). Control experiments reveal that no obvious fluorescence change with a threshold value of 300 ("false" or "0" output) is observed for other input combinations, consistent with the operation of a concatenated YES-AND-AND logic gates. The corresponding truth table is presented in Figure S9C. Moreover, the concatenated logic circuits also exhibit excellent sequence specificity, which is able to distinguish the inputs with only one-base mismatch (Figure S10). The concatenated logic circuits are then extended to develop a HB-HCR-based biomolecular keypad lock for a biocomputing security system. This system is controlled by three single-stranded DNA molecules which should be inputted in the correct order (see the Supporting Information for details).

In conclusion, we have successfully demonstrated the concept of HB-HCR through a cascade of toehold-mediated strand displacement reactions, which consists of only six DNA species and is self-sustained upon exposure to an initiator DNA strand. The chain-branching growth allows reliable differentiation between 10^{-8} equivalents and 0 equivalents of DNA initiator within 30 min, providing ultrahigh sensitivity for target DNA detection with signal amplification. Thus, the HB-HCR has great potential to become an attractive enzyme-free and isothermal alternative to the polymerase chain reaction (PCR) technique. Importantly, the proposed HB-HCR principle has been readily extended to the preparation of concatenated logic circuits with high specificity and keypad lock operations. Given the versatility of DNA when combined with aptamers or nanomaterials, the ultrasensitive and homogeneous HB-HCR system would offer a powerful platform for a wide range of applications in bioanalysis, DNA nanotechnology and nanomedicine, and in biocomputation.

Keywords: DNA structures · hybridization chain reaction · logic gates · molecular devices · self-assembly

How to cite: *Angew. Chem. Int. Ed.* **2015**, *54*, 8144–8148
Angew. Chem. **2015**, *127*, 8262–8266

[1] a) F. Wang, C.-H. Lu, I. Willner, *Chem. Rev.* **2014**, *114*, 2881–2941; b) O. I. Wilner, I. Willner, *Chem. Rev.* **2012**, *112*, 2528–2556.
[2] R. M. Dirks, N. A. Pierce, *Proc. Natl. Acad. Sci. USA* **2004**, *101*, 15275–15278.
[3] a) J. Huang, Y. Wu, Y. Chen, Z. Zhu, X. Yang, C. J. Yang, K. Wang, W. Tan, *Angew. Chem. Int. Ed.* **2011**, *50*, 401–404; *Angew. Chem.* **2011**, *123*, 421–424; b) J. Zheng, Y. Hu, J. Bai, C. Ma, J. Li, Y. Li, M. Shi, W. Tan, R. Yang, *Anal. Chem.* **2014**, *86*, 2205–2212.
[4] G. Zhou, M. Lin, P. Song, X. Chen, J. Chao, L. Wang, Q. Huang, W. Huang, C. Fan, X. Zuo, *Anal. Chem.* **2014**, *86*, 7843–7848.
[5] a) H. M. T. Choi, J. Y. Chang, L. A. Trinh, J. E. Padilla, S. E. Fraser, N. A. Pierce, *Nat. Biotechnol.* **2010**, *28*, 1208–1212; b) H. M. T. Choi, V. A. Beck, N. A. Pierce, *ACS Nano* **2014**, *8*, 4284–4294.
[6] G. Zhu, J. Zheng, E. Song, M. Donovan, K. Zhang, C. Liu, W. Tan, *Proc. Natl. Acad. Sci. USA* **2013**, *110*, 7998–8003.
[7] a) S. Venkataraman, B. M. Dirks, P. W. K. Rothemund, E. Winfree, N. A. Pierce, *Nat. Nanotechnol.* **2007**, *2*, 490–494; b) Z. Nie, P. Wang, C. Tian, C. Mao, *Angew. Chem. Int. Ed.* **2014**, *53*, 8402–8405; *Angew. Chem.* **2014**, *126*, 8542–8545; c) J. P. Sadowski, C. R. Calvert, D. Y. Zhang, N. A. Pierce, P. Yin, *ACS Nano* **2014**, *8*, 3251–3259.
[8] P. Yin, H. M. T. Choi, C. R. Calvert, N. A. Pierce, *Nature* **2008**, *451*, 318–322.
[9] H. Chandran, A. Rangnekar, G. Shetty, E. A. Schultes, J. H. Reif, T. H. LaBean, *Biotechnol. J.* **2013**, *8*, 221–227.
[10] F. Xuan, I.-M. Hsing, *J. Am. Chem. Soc.* **2014**, *136*, 9810–9813.
[11] a) C. Jung, A. D. Ellington, *Acc. Chem. Res.* **2014**, *47*, 1825–1835; b) T. Li, F. Lohmann, M. Famulok, *Nat. Commun.* **2014**, *5*, 4940–4947; c) D. Han, H. Kang, T. Zhang, C. Wu, C. Zhou, M. You, Z. Chen, X. Zhang, W. Tan, *Chem. Eur. J.* **2014**, *20*, 5866–5873; d) H. Pei, L. Liang, G. Yao, J. Li, Q. Huang, C. Fan, *Angew. Chem. Int. Ed.* **2012**, *51*, 9020–9024; *Angew. Chem.* **2012**, *124*, 9154–9158.
[12] a) J. Elbaz, O. Lioubashevski, F. Wang, F. Remacle, R. D. Levine, I. Willner, *Nat. Nanotechnol.* **2010**, *5*, 417–422; b) W. Li, Y. Yang, H. Yan, Y. Liu, *Nano Lett.* **2013**, *13*, 2980–2988; c) A. J. Genot, J. Bath, A. J. Turberfield, *J. Am. Chem. Soc.* **2011**, *133*, 20080–20083; d) F. Lohmann, H. Weigandt, J. Valero, M. Famulok, *Angew. Chem. Int. Ed.* **2014**, *53*, 10372–10376; *Angew. Chem.* **2014**, *126*, 10540–10544.
[13] a) X.-J. Jiang, D. K. P. Ng, *Angew. Chem. Int. Ed.* **2014**, *53*, 10481–10484; *Angew. Chem.* **2014**, *126*, 10649–10652; b) J. Chen, S. Zhou, J. Wen, *Angew. Chem. Int. Ed.* **2015**, *54*, 446–450; *Angew. Chem.* **2015**, *127*, 456–460.

[14] a) D. Y. Zhang, A. J. Turberfield, B. Yurke, E. Winfree, *Science* **2007**, *318*, 1121 – 1125; b) D. Y. Zhang, R. F. Hariadi, H. M. T. Choi, E. Winfree, *Nat. Commun.* **2013**, *4*, 1965 – 1974.
[15] a) See Ref. [3a]; b) F. Wang, J. Elbaz, R. Orbach, N. Magen, I. Willner, *J. Am. Chem. Soc.* **2011**, *133*, 17149 – 17151; c) S. Shimron, F. Wang, R. Orbach, I. Willner, *Anal. Chem.* **2012**, *84*, 1042 – 1048.

Received: February 14, 2015
Revised: April 24, 2015
Published online: May 26, 2015